



Royal Netherlands Institute for Sea Research

This is a postprint of:

Fan, H., Bolhuis, H. & Stal, L. (2015). Denitrification and the denitrifier community in coastal microbial mats. *FEMS Microbiology Ecology*, 91(3), 11 pp.

Published version: dx.doi.org/10.1093/femsec/fiu033

Link NIOZ Repository: www.vliz.be/nl/imis?module=ref&refid=246525

[Article begins on next page]

The NIOZ Repository gives free access to the digital collection of the work of the Royal Netherlands Institute for Sea Research. This archive is managed according to the principles of the [Open Access Movement](#), and the [Open Archive Initiative](#). Each publication should be cited to its original source - please use the reference as presented.

When using parts of, or whole publications in your own work, permission from the author(s) or copyright holder(s) is always needed.

1 DENITRIFICATION AND THE DENITRIFIER COMMUNITY IN COASTAL
2 MICROBIAL MATS

3 Haoxin Fan¹, Henk Bolhuis¹, and Lucas J. Stal^{1,2}

4 ¹Department of Marine Microbiology, Royal Netherlands Institute of Sea Research,
5 Yerseke, The Netherlands

6 ²Department of Aquatic Microbiology, Institute of Biodiversity and Ecosystem
7 Dynamics, University of Amsterdam, The Netherlands

8

9 Running head: Denitrification in a coastal microbial mat.

10

11

12 Correspondence: Lucas J. Stal, Department of Marine Microbiology, Royal Netherlands

13 Institute for Sea Research, PO Box 140, 4400 AC Yerseke, The Netherlands. Tel.: +31

14 113 577 497; Fax: +31 113 573 616

15 E-mail: Lucas.Stal@nioz.nl

16 Keywords: Denitrification, microbial mat, *nirK*, *nirS*

17

18 Abstract

19 Denitrification was measured in three structurally different coastal microbial mats by
20 using the stable isotope technique. The composition of the denitrifying community was
21 determined by analyzing the nitrite reductase (*nirS* and *nirK*) genes using clone libraries
22 and the GeoChip. The highest potential rate of denitrification ($7.0 \pm 1.0 \text{ mmol N m}^{-2} \text{ d}^{-1}$)
23 was observed during summer at station 1 (supra-littoral). The rates of denitrification were
24 much lower in the stations 2 (marine) and 3 (intermediate) (respectively 0.1 ± 0.05 and
25 $0.7 \pm 0.2 \text{ mmol N m}^{-2} \text{ d}^{-1}$) and showed less seasonality when compared to station 1. The
26 denitrifying community at station 1 was also more diverse than that at station 2 and 3,
27 which were more similar to each other than either of these stations to station 1. In all
28 three stations, the diversity of both *nirS*- and *nirK*-denitrifiers was higher in summer
29 when compared to winter. The location along the tidal gradient seems to determine the
30 composition, diversity and activity of the denitrifier community, which may be driven by
31 salinity, nitrate/nitrite and organic carbon. Both *nirS* and *nirK* denitrifiers are equally
32 present and therefore they are likely to play a role in the denitrification of the microbial
33 mats studied.

34

35

36 Introduction

37 Denitrification is a bacterial process during which nitrate or nitrite is stepwise reduced
38 through a few intermediate gaseous nitrogen compounds to dinitrogen (Zumft, 1997).

39 Nitrite reductase is present in all denitrifying bacteria and mediates the reduction of
40 nitrite to nitric oxide and is considered as the key enzyme of denitrification. There are
41 two functional equivalent but structurally distinct nitrite reductases known in denitrifying
42 bacteria (Zumft, 1997). These are Cytochrome cd1 (Cd-Nir), encoded by *nirS* and a
43 copper nitrite reductase (Cu-Nir), encoded by *nirK*. There are no organisms known that
44 carry both genes and therefore these two enzymes are thought to be mutually exclusive
45 (Zumft, 1997). Nitrite reductase genes have been used as functional molecular markers
46 for denitrification in natural environments and have revealed the diversity of denitrifying
47 bacteria in a variety of habitats such as soil (Prieme *et al.*, 2002; Throbäck *et al.*, 2007),
48 estuarine sediments (Santoro *et al.*, 2006), marine sediments (Braker *et al.*, 2000; Hannig
49 *et al.*, 2006), and seawater (Castro-Gonzalez *et al.*, 2005; Jayakumar *et al.*, 2004; Oakley
50 *et al.*, 2007). Environmental factors were identified that shaped the denitrifier community
51 composition (Braker *et al.*, 2000; Hallin *et al.*, 2009). Moreover, the type of habitat
52 determined the presence or dominance of *nirS*- and *nirK*- type denitrifiers (Hannig *et al.*,
53 2006; Oakley *et al.*, 2007).

54

55 Coastal microbial mats are compact, highly structured, small-scale ecosystems (Stal,
56 2001). These mats are built by cyanobacteria, oxygenic phototrophic bacteria, which
57 through primary production enrich the sediment with organic matter. This organic matter
58 forms the basis of a complex, multi-layered microbial ecosystem. Previous studies of

59 nitrogen cycling in microbial mats have focused mainly on the nitrogen fixation and only
60 a few studies documented denitrification in microbial mats. Joye & Paerl (1994) studied
61 denitrification in microbial mats of Tomales Bay (California) and found that it removed
62 only 15% of the N₂ that was fixed on an annual basis in these mats. In a hypersaline
63 microbial mat, denitrification was lower than N₂ fixation in summer, but exceeded N₂
64 fixation in winter when it turned the mat into a sink for nitrogen (Bonin & Michotey,
65 2006). Desnues *et al.* (2007) reported spatio-temporal distribution of denitrifying bacteria
66 in a hypersaline microbial mat. These studies focused on the rates of denitrification and
67 did not give information on the diversity and the temporal and spatial distribution of the
68 denitrifying bacteria and their activities and therefore provided only an incomplete view
69 on this process in microbial mats.

70

71 We investigated microbial mats that proliferate at the North Sea coast of the Dutch
72 barrier island Schiermonnikoog. Based on morphological, microscopic, and molecular
73 genetic differences we distinguish three major types of microbial mats that develop along
74 the tidal gradient. The bacterial, archaeal and eukaryal community composition and
75 microbial diversity were intrinsic of the mat type and depended on the location along the
76 tidal salinity gradient (Bolhuis & Stal, 2011; Bolhuis *et al.*, 2013). Previously it was
77 shown that N₂ fixation and the diazotrophic community varied along the same lines at
78 these three stations (Severin & Stal, 2010). The variation of N₂ fixation may be
79 attributed to different environmental conditions in microbial mats, which changes
80 spatially (location along the tidal gradient) and temporally (tide, day-night, and seasonal).
81 We expect that the same factors exert also a selective force on the denitrifying

82 community and its activity. At the different positions along the tidal gradient the mats
83 would allow the development of different community compositions, which would also
84 alter the potential rate of denitrification that can be achieved (Philippot & Hallin, 2005).
85 In this study we measured the potential rates of denitrification in the three different mat
86 types during different seasons. Alongside, we identified the denitrifying communities and
87 measured relevant environmental variables in order to elucidate: 1) whether mats along
88 the tidal gradient contain different types of denitrifying bacteria; 2) whether a relationship
89 exists between the denitrifier community and the potential rate of denitrification; 3)
90 which environmental factors affect denitrification and the composition of the denitrifier
91 communities.

92

93 Material and methods

94 Study area and sampling

95 The study site was located on the North Sea coast of the Dutch barrier island
96 Schiermonnikoog. The geographical locations and descriptions of the three types of
97 microbial mats (stations) that were sampled for this study are given in Table 1. The
98 sample stations were situated along a transect perpendicular to the beach covering the
99 tidal gradient. Sampling was done at four different seasons during 2010 and 2011.
100 Samples were taken from the top 2.5-3 cm of the mat using custom-made transparent
101 Lexan cylinder cores of 50 mm inner diameter and 60 mm height. The cores were
102 transported back to the laboratory within 4 h of sampling and kept at ambient temperature
103 and light. The incubations started within 24 h after sampling. Additional samples were
104 taken for nucleic acid extraction. These samples were taken from the top 1 cm of the mat

105 by using a 10 ml truncated syringe as a corer. These mat samples were divided into four
106 equal parts, put into cryo-vials, and immediately frozen in the field in liquid nitrogen.

107

108 Chemical analyses

109 For nutrient analyses 5 g mat sample (top 1 cm) was extracted with 40 ml 2 M KCl. The
110 extracts were filtered through Whatman GF/F filters and the filtrates were kept at -20 °C
111 until analysis (within a month). Nutrient concentrations were measured on an automated
112 Segmented Flow Analyzer using standard analytical procedures. Other mat samples were
113 freeze-dried for the determination of total nitrogen (TN), total organic carbon (TOC) and
114 C/N ratio by EA-IRMS (DELTA V Advantage; Thermo Fisher Scientific, Bremen,
115 Germany).

116

117 Measurement of potential denitrification

118 Subsamples of 1.2 cm² (10 mm thickness) of the cores of the mats were placed into 12.5
119 ml Exetainers (Labco Limit, Buckinghamshire, England) by using a 5-ml syringe as a
120 corer. The measurements were carried out according to Thamdrup & Dalsgaard (2002)
121 with some modifications. Briefly, the Exetainers were completely filled with anoxic
122 artificial seawater (NaCl 20.5 g, Na₂SO₄ 3.4 g, KCl 0.58 g, KBr 0.084 g and H₃BO₃
123 0.022 g, MgCl₂·6H₂O 0.05 mol, CaCl₂·2H₂O 0.01 mol in 1000 ml Milli-Q water).

124 Addition of 100 μM Na¹⁵NO₃ (98.5%, ¹⁵N atom%; Sigma-Aldrich, 100 μM ¹⁵NH₄Cl
125 (99.2%, ¹⁵N atom%; Sigma-Aldrich) and 100 μM ¹⁵NH₄Cl + 100 μM Na¹⁴NO₃ were
126 applied to the Exetainers, respectively. Before the addition of the ¹⁵N tracer, the
127 Exetainers were placed in dark for 2 h to allow the depletion of NO_x⁻ and any residual

128 oxygen. All Exetainers, including one set without any addition, were incubated for 24 h
129 in the dark at ambient temperature (Table 2). At 4-h intervals during 24 h two replicate
130 Exetainers from each treatment were fixed by injecting 200 μ l 50% (w/v) ZnCl₂. The
131 Exetainers were stored at 4°C in the dark upside down until analysis (within a week). The
132 isotopic composition of the dinitrogen of He-equilibrated headspace (2 ml in the 12.5-ml
133 Exetainer vials) was determined by an EA-IRMS (DELTA V Advantage; Thermo Fisher
134 Scientific, Bremen, Germany) equipped with a Haysep Q column. The potential rate of
135 denitrification was calculated from the linear production of excess ²⁹N₂ and ³⁰N₂
136 according to Thamdrup & Dalsgaard (2002).

137

138 DNA extraction, PCR, cloning and sequencing

139 DNA was extracted using the MoBio UltraCLEAN soil DNA kit (MoBio Laboratories,
140 Inc., Carlsbad, CA, USA) according to the manufacturer's instructions. Fragments of the
141 genes *nirS* and *nirK* were amplified using the primer pairs cd3aF-R3cd for *nirS* and
142 F1aCu-R3Cu for *nirK* (Throbäck *et al.*, 2004). PCR conditions for the two sets of primer
143 pairs were 2 min at 95°C, 35 cycles of 50 sec 95°C, 50 sec 53°C, and 50 sec at 72°C,
144 followed by a final extension of 10 min at 72°C. PCR products were checked on a 1%
145 agarose gel. PCR products were cloned using the TOPO-TA cloning kit with the pcR2.1
146 vector and TOP10 competent cells (Invitrogen, Carlsbad, CA, USA) following the
147 manufacturer's instructions. Transformants were randomly picked from each clone
148 library and screened by PCR using T3 and T7 vector primers following the recommended
149 PCR conditions (Invitrogen, Carlsbad, CA, USA). Forty-eight clones were randomly
150 selected for sequencing with the T7 vector primer using ABI PRISM 3130 Genetic

151 Analyzer (Applied Biosystems, Foster City, CA, USA). The total number of sequences
152 obtained from each clone library varied (28-70 sequences) due to the variable quality of
153 the sequencing reads. Sequences have been submitted to NCBI (accession numbers
154 KJ738332 - KJ739305).

155

156 Sequence analysis

157 Sequences were edited, aligned and translated using MEGA 5 (Molecular Evolutionary
158 Genetics Analysis, <http://www.megasoftware.net/mega5/mega.html>) and manually
159 checked. Neighbor-joining trees were produced and the reliability of the phylogenetic
160 reconstructions was evaluated by bootstrapping (1000 replicates). The program Mothur
161 (http://www.mothur.org/wiki/Main_Page) was used to calculate the non-parametric
162 richness estimators and the Shannon diversity index and to determine the differences in
163 nucleic acid sequences. Operational Taxonomic Units (OTUs) were defined by a 5%
164 difference in nucleic acid sequence for the purpose of community analysis. Based on the
165 OTUs from each library, sequence data were transformed into binary data
166 (presence/absence) for community composition analysis.

167

168 GeoChip analysis

169 The GeoChip is a high-throughput functional gene array covering 289 functional gene
170 families involved in the biogeochemical cycling of carbon, nitrogen, phosphorus and
171 sulfur (He *et al.*, 2010). For the analysis using the GeoChip we used DNA extracted in
172 triplicate from the three types of microbial mats sampled in July and in November. The
173 DNA was purified using UltraClean 15 DNA purification Kit (MoBio Laboratories, Inc.,

174 Carlsbad, CA, USA) in order to achieve the quality necessary for hybridization on the
175 chip. The DNA quantity was measured by an ND-1000 spectrophotometer (Nanodrop
176 Inc., Wilmington, DE). The procedures for DNA labeling and microarray hybridization
177 followed the previously established protocols (Wu *et al.*, 2006). Briefly, 800 ng of
178 environmental DNA was labeled with fluorescent dye Cy-5 by random priming. The
179 labeled DNA was re-suspended in 50 μ l hybridization solution [40% formamide, 5 x
180 SSC, 5 μ g of unlabeled herring sperm DNA (Promega, Madison, WI), and 0.1% SDS]
181 and 2 μ l universal standard DNA (0.2 pmol μ l⁻¹) labeled with the fluorescent dye Cy-3
182 (Liang *et al.*, 2010), denatured at 95°C for 5 min and maintained at 50°C until loaded
183 onto the microarray slides. Arrays were hybridized on a MAUI Hybridization Station
184 (Roche, South San Francisco, CA) for 12 h at 42°C. Hybridized microarrays were
185 scanned by a ScanArray Express Microarray scanner (Perkin-Elmer, Wellesley, MA) at
186 95% laser power and 85% photomultiplier tube gain. The resulting images were analyzed
187 by ImaGene with signals processed as SN>2.0 (signal to noise ratio).

188

189 Statistical analysis

190 In order to summarize the gene overlap at station and season level, the detected genes
191 from the GeoChip in the three replicates of each station from July and November were
192 deployed as one pool (mean value from the three replicates). The analyses of overlapping
193 genes, unique genes, and diversity indices were performed using an online pipeline
194 (<http://ieg.ou.edu/>). The proportion of overlapping genes was calculated as the number of
195 overlapping genes divided by the total number of genes detected in both stations. The

196 proportion of unique genes at each station was calculated as the number of unique genes
197 at each station divided by the total number of genes detected at that station.

198 Statistical analyses of the multi-response permutation procedure (MRPP) and canonical
199 correspondence analysis (CCA) (see below) were performed based on community data
200 from the clone libraries as well as from the GeoChip data. MRPP using Bray-Curtis
201 distance was used to test for significant differences in community composition. The
202 MRPP A-statistics describes the within and between group relatedness relative to what is
203 expected by chance. A p-value <0.05 and an A-statistics >0.1 is considered as significant
204 difference between groups (McCune *et al.*, 2002). To test the relationship between the
205 denitrifier community and the environmental variables, CCA was carried out. The
206 significance of the whole canonical model was tested by 999 permutations. All statistical
207 analyses were carried out in the open source-software R (Team, 2011), using the vegan
208 package (Oksanen, 2011). Stepwise regression was carried out to test the influence of the
209 environmental factors and denitrifier community on potential denitrification rates using
210 SigmaPlot (SigmaPlot, Version 12). Denitrifier communities were converted into
211 univariate variables based on the sample scores for the first two CCA axes.

212

213 Results

214 Physicochemical characteristics

215 Table 2 lists the seasonal and annual mean values of the physicochemical parameters of
216 the sample sites and the potential denitrification rates in the three mats. The
217 physicochemical parameters fluctuated seasonally and some parameters showed
218 differences between the three mat types. Ammonium concentration was lowest at Station
219 1 (ST1) and highest at ST3, except in April. Nitrate/nitrite concentrations were in the
220 same range at all stations, albeit with slightly higher concentrations in July and April and
221 slightly lower concentrations in September and January. Phosphate concentration was
222 highest in April and lowest in September at all stations. TOC and TN were similar at ST2
223 and ST3 but always lowest at ST1.

224

225 Potential denitrification rates

226 $^{29}\text{N}_2$ and $^{30}\text{N}_2$ were produced at the expected ratio for denitrification given the addition of
227 99.2-atom% enriched $^{15}\text{NO}_3^-$. Denitrification rates (N_2 production) showed remarkable
228 differences between the three stations and varied also seasonally. For ST1 (supratidal,
229 close to the dunes) the potential denitrification rates ranged from 0.1 ± 0.05 - 7.0 ± 1.0
230 $\text{mmol N m}^{-2}\text{d}^{-1}$ (Table 2). The denitrification rate was highest in July ($7.0 \pm 1.0 \text{ mmol N m}^{-2}$
231 d^{-1}) and much lower ($1.6 \pm 0.3 \text{ mmol N m}^{-2}\text{d}^{-1}$) in September. Denitrification was lowest
232 ($0.1 \pm 0.05 \text{ mmol N m}^{-2}\text{d}^{-1}$) in April. The seasonal trend of denitrification at the littoral site
233 (ST3) was slightly different from that at ST1. At ST3, the highest denitrification rate
234 ($0.7 \pm 0.2 \text{ mmol N m}^{-2}\text{d}^{-1}$) was in July and was lowest in September ($0.1 \pm 0.05 \text{ mmol N m}^{-2}$
235 d^{-1}). A higher rate ($0.5 \pm 0.2 \text{ mmol N m}^{-2}\text{d}^{-1}$) was again observed during January. Unlike

236 the other two sites, the highest rate of denitrification at ST2 (low water mark) (1.6 ± 0.4
237 $\text{mmol N m}^{-2}\text{d}^{-1}$) was observed in January and the lowest rate (0.1 ± 0.05 $\text{mmol N m}^{-2}\text{d}^{-1}$)
238 occurred in July and September. The annual average denitrification rate was highest at
239 the supra-littoral (near the dunes, ST1) (2.8 $\text{mmol N m}^{-2}\text{d}^{-1}$) and significantly higher
240 ($P < 0.05$) than at the other two stations, which were low and not significantly different
241 from each other (0.5 $\text{mmol N m}^{-2}\text{d}^{-1}$ at ST2 and 0.4 $\text{mmol N m}^{-2}\text{d}^{-1}$ at ST3).

242

243 *nirS* and *nirK* diversity and composition

244 *nirS* and *nirK* sequences from the three stations were analyzed. Combining the clone
245 libraries, 76 unique *nirS* operational taxonomic units (OTUs) and 74 unique *nirK* OTUs
246 (at a 5% distance cut-off) were retrieved. The richness and diversity estimators showed
247 different *nirS* and *nirK* gene richness at the three stations. *nirS*-denitrifier community was
248 richest at ST3, while the other two stations showed a similar richness. *nirK*-denitrifier
249 community was richest at ST1 and poorest at ST3.

250

251 Phylogenetic analyses of deduced amino acid sequences for *nirS* and *nirK* gene fragments
252 are shown in Fig. 1. The *nirS* sequences clustered into three distinct groups (Fig. 1A).
253 Group I contained 53%, 36% and 68% of the total sequences from ST1, ST2 and ST3,
254 respectively. The sequences in this group were closely related to the cultivated denitrifier
255 *Marinobacter* sp. U31 (CAF25138) as well as to environmental clones from a
256 hypersaline microbial mat (e.g. CAL69009, CAL69007), an estuarine sediment (e.g.
257 AEK77712, ABY52470) and from the Baltic Sea (e.g. CAJ87449). Group II contained
258 12%, 64% and 30% sequences from ST1, ST2 and ST3, respectively. Sequences in

259 Group II clustered closely with those of a variety of cultivated denitrifiers including
260 *Roseobacter denitrificans*, *Paracoccus denitrificans*, and *Silicibacter pomeroyi*. The third
261 group contained 35% and 2% of the sequences of ST1 and ST3. These sequences were
262 closely related to *Pseudomonas stutzeri*, *Azospirillum brasilense* and *Ralstonia eutropha*.
263
264 *nirK* sequences clustered into four groups (Fig. 1B). Group I contained 2%, 81% and
265 100% of the total *nirK* sequences from ST1, ST2 and ST3, respectively. The sequences
266 belonging to group I were most closely related to environmental clones from San
267 Francisco Bay estuarine sediment (ADM93883) and from the Arabian Sea oxygen
268 minimum zone (ACT98741). Three OTUs from ST1 fell into Group II, showing the best
269 hit of 87% nucleotide sequence similarity with a sequence retrieved from a Chinese
270 agricultural soil (HM628810). Group III contained sequences from ST1 (7%; 17%; 68%,
271 Fig. 1B) and were related to a variety of cultivated denitrifiers, such as *Rhodobacter*
272 *sphaeroides* (CCA12211) and *Rhodopseudomonas palustris* (NP949481). Group IV
273 comprised only sequences (19%) from ST2. These sequences are closely related to
274 environmental clones from San Francisco Bay estuarine sediment (ADM93844,
275 ADM93870) and remotely related to the cultivated *Alcaligenes* sp. (75% similarity and
276 48% sequence coverage).
277
278 Diversity of *nirS* and *nirK* genes based on GeoChip analysis is summarized in Table 4. A
279 total of 264 *nirS* sequences showed a hybridization signal in at least one of mat. The
280 average number of *nirS* sequences (richness) at ST1 (July), ST2 (July), ST3 (July), ST1
281 (January), ST2 (January) and ST3 (January) was 253, 206, 146, 215, 161, and 125,

282 respectively (Table 4). Thirty-three sequences were unique and detected only at one of
283 the stations and during one season. In July, ST1 harbored 26 unique sequences, which
284 was 10.3% (26/253) of the total number detected. ST2 and ST3 harbored 2.4% (5/206)
285 and 0.7% (1/146) unique sequences, respectively. In January, the number of unique
286 sequences in ST1 dropped to 3, which was only 1.4% (3/215) of the total number
287 detected. In January no unique sequences were observed at ST2 and ST3. Pairwise
288 comparison of *nirS* sequences showed a high number of overlapping *nirS* sequences
289 between summer and winter as well as between the stations: 81% (ST1 July & January),
290 72% (ST2 July & January), 70% (ST3 July & January), 74-77% (ST1&ST2), 57%
291 (ST1&ST3) and 68-70% (ST2&ST3).

292

293 Similar results were obtained for *nirK* (Table 4). We detected 264 *nirK* sequences in the
294 mats. Most *nirK* sequences were detected in summer at ST1 (256). We detected 204, 141,
295 214, 150 and 127 *nirK* sequences at ST2 (July), ST3 (July) ST1 (January), ST2 (January)
296 and ST3 (January), respectively (Table 4). In July, ST1 harbored 26 unique sequences,
297 which was 10.2% (26/256) of the total detected sequences. ST2 and ST3 harbored 1.5%
298 (3/204) and 0.7% (1/141) unique sequences of the total detected number, respectively. In
299 January, only 1 unique sequence was detected both at ST1 and ST2. No unique sequence
300 was detected at ST3. Seventy-seven percent of the total detected *nirK* sequences were
301 shared by ST1 and ST2, 54% was shared by ST1 and ST3 and 67% was shared by ST2
302 and ST3.

303

304 The diversity indices for *nirS* and *nirK* were assessed by richness and Shannon-Weaver
305 index (Table 4). At all stations the values for both diversity estimators were higher in
306 summer. The highest richness was observed in summer at ST1 and the lowest value was
307 found in summer and winter at ST3 ($p < 0.01$). The highest abundance for both *nirS* and
308 *nirK* were observed in summer at ST1. The lowest abundance for *nirS* was found at ST3
309 and for *nirK* was found in summer at ST2 and winter at ST3.

310

311 Multi-response permutation procedure (MRPP) statistics was carried out to test the
312 differences of the composition of the microbial community between the stations based on
313 *nirS* and *nirK* OTUs obtained from the clone libraries and the GeoChip. MRPP testing of
314 these two data sets gave consistent results. Distinctly different denitrifier communities
315 were found in ST1 when compared to the other two stations ($p < 0.05$) from the two data
316 sets. ST2 and ST3 did not contain significantly different communities ($p > 0.05$) when the
317 analysis was based on data from the GeoChip but were significantly different when using
318 the data from the clone libraries ($p > 0.05$). This was the case for both *nirS* and *nirK* (Table
319 5). There were no seasonal differences in the denitrifier communities in any of the
320 stations (data not shown). These results were confirmed by CCA analyses (Fig. 2).

321

322 Environmental control of denitrifying mat community and activity

323 No relationship between potential denitrification rates, environmental factors, and the
324 denitrifier community were revealed based on stepwise regression analysis. Canonical
325 correspondence analysis (CCA) was applied in order to discover patterns in the
326 composition of the denitrifying community. Using CCA we analyzed the *nirS* and *nirK*

327 sequence data obtained from the clone libraries and from the GeoChip with the related
328 environmental factors (Table 2).

329

330 Figure 2A shows the results of the CCA from the *nirS* sequences obtained from clone
331 libraries. In the diagram, denitrifiers were distinctly grouped according to sample station.
332 There was no effect of the season. The community composition was significantly
333 correlated with all selected variables in the adapted CCA model ($p=0.02$) (based on 999
334 permutations test). In the CCA diagram (Fig. 2A), the first two axes explained 71% of
335 relationship between the total *nirS* containing community and the environmental factors.
336 The first canonical axis explained 42.5% of total variations ($p=0.008$) and was dominated
337 by the environmental variables TOC ($p<0.05$), TN, and ammonium concentration
338 ($p<0.05$). The second canonical axis explained an additional 28.5% of the constrained
339 variations and was dominated by phosphate ($p<0.05$) and the nitrate+nitrite
340 concentration. The *nirS* containing community in ST1 was distinctly different from those
341 in ST2 and ST3 along the first canonical axis (Axis 1), while the *nirS* containing
342 communities in ST2 and ST3 separated along the second canonical axis (Axis 2). ST2
343 and ST3 were influenced by both the first and second canonical axes and positively
344 correlated with TOC ($p<0.05$), TN, phosphate ($p<0.05$) and ammonium concentrations
345 ($p<0.05$), but negatively correlated with nitrate+nitrite concentration ($p<0.05$). ST1 was
346 primarily influenced by the first canonical axis, reflecting the role of TOC ($p<0.05$), TN,
347 and ammonium concentrations ($p<0.05$). For each individual variable, a significant
348 correlation was found between community and TOC ($r^2=0.89$, $p=0.003$) and TN ($r^2=0.87$,
349 $p=0.003$), which is indicated by the length of the arrows in the CCA diagram.

350

351 Figure 2B shows the CCA profiles based on the seasonal *nirS* community data as
352 obtained from the GeoChip. GeoChip analyses were only performed on the summer and
353 winter samples. Spatially, *nirS* communities from different stations were separated along
354 the first axis of the CCA diagram. Temporally, *nirS* communities of the summer samples
355 were separated from those of the winter samples along the second axis. In general, the
356 community composition was significantly correlated with all selected variables in the
357 adapted CCA model ($p=0.001$) (based on 999 permutations test). Due to
358 multicollinearity, the C:N ratio, salinity and the potential rate of denitrification were
359 removed. Therefore, five environmental factors were selected and are depicted in the
360 diagram. The first two axes explained 47.7% of the relationship between the total *nirS*
361 community composition and the environment. The first canonical axis explained 33.4%
362 of the total variation ($p=0.001$). The first axis was dominated by the environmental
363 variables TOC ($p<0.001$), TN ($p<0.001$) and ammonium concentration ($p<0.001$). The
364 second axis explained the rest 14.4% of the total variation ($p=0.001$) and was dominated
365 by phosphate ($p<0.001$) and the nitrate+nitrite concentration ($p<0.001$). For ST1, the
366 *nirS* community was influenced by all factors taken into account and showed negative
367 correlation with TOC, TN and ammonium concentration. The *nirS* containing community
368 in the summer samples correlated positively with nitrate+nitrite and phosphate
369 concentrations, while the community in the winter samples was negatively correlated
370 with these factors. For ST2, *nirS* in the summer samples was only influenced by the
371 factors reflected by second axis. The *nirS* community in the winter samples was
372 influenced by all the selected factors and was positively correlated with TOC, TN and

373 ammonium concentrations but negatively correlated with phosphate ($p < 0.001$) and
374 nitrate+nitrite concentrations. For ST3, the *nirS* community was positively correlated
375 with TOC, TN and ammonium concentrations. The *nirS* in the summer samples also
376 showed a positive correlation with phosphate ($p < 0.001$) and nitrate+nitrite concentrations
377 (although this was not significant), while *nirS* in the winter samples was not strongly
378 influenced by any of the environmental variables on the second axis.

379

380 Figure 2C and 2D depict the results of the CCA from the *nirK* containing communities.
381 For both the cloning and GeoChip data, the first two axes explained the community
382 composition better than the observations of the *nirS* containing community. The axes 1
383 and 2 explained 72.1 and 51.7% of the total variation of the *nirK* containing community,
384 respectively. The *nirS* and *nirK* containing communities responded similarly to spatial
385 and temporal variation of the environmental factors.

386

387

388

389 Discussion

390 The few existing studies on denitrification in microbial mats used the acetylene inhibition
391 technique (AI). The published rates of denitrification in microbial mats ranged from 0 to
392 3.14 mmol N m⁻² d⁻¹ (Bonin & Michotey, 2006; Desnues *et al.*, 2007; Joye & Paerl,
393 1994). In the present study, we measured potential denitrification rates by the isotope
394 pairing (IP) technique using small cores of the mat from 0.06 to 7.00 mmol N m⁻² d⁻¹ and,
395 hence, were in the same range. We do realize that such comparisons fall short because of
396 differences that are inherent of the technique as well as different incubations (i.e. intact
397 cores *versus* slurries). E.g. Lohse *et al.* (1996) concluded that the AI technique
398 underestimated the rate of denitrification by a factor of two when compared to the IP
399 technique. Also Bonin & Michotey (2006) measured denitrification in a microbial mat in
400 the Camargue using both the AI and IP techniques and found that the latter gave 10-fold
401 higher rates. However, the AI technique is not adequate when denitrification depends on
402 nitrification in the sediment, because acetylene blocks the latter. Our measurements did
403 not depend on nitrification since we added ample nitrate.

404

405 A previous study on the same mats revealed that in summer nitrogen fixation was 2.0, 0.5
406 and 2.1 mmol N m⁻² d⁻¹ for the stations 1, 2 and 3, respectively (Severin & Stal, 2008).
407 Similar mats on the German Wadden Sea barrier island Mellum fixed 3.2, 0.2 and 1.0
408 mmol N m⁻² d⁻¹ for the stations that were representative for those studied here (station 1,
409 2 and 3, respectively) (Stal *et al.*, 1984). Hence, these values indicate that denitrification
410 and N₂ fixation are in the same range in the coastal mats studied here. Joye & Paerl
411 (1994) measured denitrification by the AI technique and showed that denitrification was

412 only 15% of N₂ fixation on an annual basis in the mats of Tomales Bay. However, given
413 that denitrification is underestimated by the AI technique, denitrification may have been
414 responsible for a much higher proportion of the loss of the fixed N₂. Also, Bonin &
415 Michotey (2006) found that denitrification exceeded N₂ fixation in winter in the
416 hypersaline mat in Camargue. Hence, we conclude that denitrification can be an
417 important sink for the fixed nitrogen in microbial mats.

418

419 Spatial and temporal heterogeneity of potential denitrification rates were observed in the
420 present study and have also been documented for other microbial mats (Bonin &
421 Michotey, 2006; Joye & Paerl, 1994). ST1 and ST3 showed the highest potential
422 denitrification rates in summer (July), which was consistent with what has been reported
423 for the hypersaline mats in the Camargue (Bonin & Michotey, 2006) and for the mudflat
424 mats in Tomales Bay (Joye & Paerl, 1994). These results suggest that the nitrogen cycle
425 in different phototrophic microbial mats behaves in a similar way. This might be due to
426 the fact that microbial processes in phototrophic microbial mats are fundamentally the
427 same and driven by the physicochemical gradients typically existing in these ecosystems
428 (Stal, 2012).

429

430 The potential rate of denitrification in each of the mats can most likely be attributed to the
431 dissimilar denitrifier communities. Denitrifiers are phylogenetically diverse and therefore
432 it is expected that the physiology and enzyme affinities may vary considerably (Philippot
433 & Hallin, 2005). Consequently, shifts in community composition would lead to changes

434 in the potential rate of denitrification and this has actually been shown in several cases
435 (Cavigelli&Robertson, 2000; Jayakumar et al., 2004; Rich et al., 2003).

436 We used GeoChip and clone libraries to investigate the denitrifier community in
437 microbial mats. Clone libraries offer the possibility to discover novel species of
438 denitrifiers (assessed by evaluating and analyzing the *nirS* and *nirK* genes) in the
439 microbial mats. However, the limited numbers of clones that were sequenced and the bias
440 of the PCR approach targeting mainly dominant groups could have underestimated the
441 rare types. Therefore we used in addition the GeoChip. This chip provides a high
442 coverage of the *nirS* and *nirK* genes that are not sufficient abundant to be retrieved by
443 clone libraries, provided that their probes were included on the chip. The combination of
444 these two approaches allowed us to obtain a comprehensive diversity of the *nirS*- and
445 *nirK*-denitrifiers in the microbial mats. The results from both analyses were in agreement
446 with each other.

447

448 The phylogenetic analysis of the denitrifier community using *nirS* and *nirK* revealed that
449 denitrifiers inhabited all three types of microbial mats. Most of the *nirS* and *nirK* genes
450 retrieved in this study were unrelated to known denitrifying bacteria but shared
451 considerable phylogenetic similarity with sequences from diverse environments including
452 estuarine (Santoro *et al.*, 2006), marine habitats (Castro-Gonzalez *et al.*, 2005) as well as
453 soil (Throbäck *et al.*, 2007) and sludge (Osaka *et al.*, 2006). This suggests that a large
454 number of the denitrifiers in these microbial mats have not yet been cultivated. The high
455 diversity of the denitrifier community may be due to a variety of potential environmental
456 niches present in the microbial mats, which would allow diverse denitrifiers to

457 proliferate. The deduced amino acid sequences of *nirS* and *nirK* fragments retrieved from
458 clone libraries made from each of the sample stations were more similar to each other
459 than to those of the other stations and hardly overlapped with the sequences from other
460 stations. Although the *nirS* phylogenetic tree did not show a clear division of the clones
461 according to the stations from which they originated, as was the case for the *nirK* tree,
462 CCA analyses confirmed that both *nirS*- and *nirK*-denitrifier communities partitioned
463 according to the different mat types. This shows that the conditions that prevail in a
464 certain mat type selects for the type of denitrifier. This is in agreement with a clone
465 library based study of a denitrifier community along a salinity and nitrate gradient in a
466 coastal aquifer. Santoro and coworkers found that both NirS and NirK were distinct for
467 certain communities, exhibiting little overlap between stations (Santoro *et al.*, 2006). This
468 habitat specificity of *nirS*- and *nirK*- denitrifier communities was observed in various
469 other environments such as the Baltic Sea and freshwater lakes (Kim *et al.*, 2011) or soils
470 (Prieme *et al.*, 2002).

471

472 Diversity estimates (Shannon-Weaver) based on the clone library GeoChip indicated that
473 ST1 harbored a more diverse *nirK*-type denitrifying community than the other two
474 stations. With respect to *nirS* diversity, estimates made by clone libraries and the
475 GeoChip were not consistent and we are therefore unable to draw a conclusion for this
476 gene. The stringency of hybridization was optimized (Wu *et al.*, 2006). The group-
477 specific probes matched perfectly with their targets and the false positive signal was
478 negligible. Most unique *nirS* and *nirK* were detected at ST1 suggesting that this station is
479 different from the other two. Moreover, the phylogenetic trees of translated *nirS* and *nirK*

480 from ST2 and ST3 show that a large number of sequences fell into the same clusters,
481 suggesting that the denitrifying communities of these two stations were similar. The *nirS*
482 and *nirK* sequences from ST1 formed distinct clusters. Multi-response permutation
483 procedure analysis based on clone libraries and GeoChip of *nirS* and *nirK* confirmed that
484 the similarity was higher between ST2 and ST3 than either of these stations to ST1.
485 Hence, in this respect the dissimilarity of the denitrifying communities in the three
486 stations did not follow the pattern of the whole microbial community (Bolhuis & Stal,
487 2011). These authors found that the microbial community of ST2 was more dissimilar
488 from that of ST1 and ST3. The *nirS*- and *nirK* denitrifiers showed higher diversity during
489 summer and a lower diversity during winter. This is in agreement with the development
490 of a mat, which grows to maturity during summer and growth stops during winter when
491 the mat is degraded (Stal *et al.*, 1985).

492

493 The spatial organization of the denitrifying community in the microbial mats was likely
494 the result of the different environmental conditions. Salinity has been proposed as the
495 major driver of the microbial community composition for these microbial mats (Bolhuis
496 *et al.*, 2013). This might also apply to the denitrifier community. Jones & Hallin (2010)
497 concluded that the global distribution pattern of *nirS* and *nirK* genes corresponded to
498 salinity. The lower salinity at ST1 may explain the higher diversity of the denitrifier
499 community. This has also been observed in a benthic denitrifier community along the
500 estuarine gradient in Chesapeake Bay (Bulow *et al.*, 2008). These authors found the
501 highest *nirS* diversity at a freshwater station and the lowest diversity at a station with
502 high salinity. Nitrite reductase genes in a wastewater treatment system showed that

503 salinity decreased the diversity of both *nirS* and *nirK* containing denitrifying bacteria
504 (Yoshie *et al.*, 2004). Similar observations have been made for other functional genes of
505 the N-cycle. Severin *et al.* (2012) investigated the same mats as in this study and found
506 that the proportion of cyanobacterial *nifH* transcripts decreased with increasing salinity.
507 Likewise, Bernhard *et al.* (2010) found that the loss of diversity of ammonia-oxidizing
508 bacteria correlated with increasing salinity in the Plum Island Sound estuary. Possible
509 factors for the denitrifier compositional changes were partly associated with but not
510 exclusively driven by salinity.

511

512 Canonical correspondence analysis of the *nirS* and *nirK* genes indicated that organic
513 substrates and nitrate/nitrite are also important environmental factors influencing the
514 denitrifier community composition but in opposite ways. Nitrite is the electron acceptor
515 in denitrification. The nitrate/nitrite concentration at ST1 was slightly higher than at the
516 other two stations and this might be the underlying reason for the different denitrifier
517 community in this station (Table 2). This is in line with the observation of Liu *et al.*
518 (2003) who found that denitrifying communities were similar when the nitrate
519 concentrations were at the same level. Organic carbon is the primary electron donor for
520 heterotrophic denitrifiers (Zumft, 1997). We showed that the highest diversity of the
521 denitrifier community was at the station with the lowest concentration of organic matter
522 (Table 2). Most of this organic matter is recalcitrant polymeric material (Stal, 2003). We
523 conceive that this would increase the diversity of denitrifiers. When organic matter is
524 available, diversity will be low because of strong competition and out-competing of the
525 less adapted species.

526

527 The two dimensions of CCA explained only part of the total variance of the denitrifier
528 community (Fig. 2). This implies that there are also other factors that contribute to the
529 composition of microbial community. For example, interaction and competition for
530 resources with other microorganisms could be additional factors. In the microbial mats,
531 denitrifiers compete for nitrate+nitrite with the primary producers such as cyanobacteria
532 and diatoms that represent dominant groups in these mats (Bolhuis & Stal, 2011; Severin
533 *et al.*, 2010). The diversity of the *nifH* gene in these mats varied in a similar way (Severin
534 & Stal, 2010). These authors found that the diazotrophic communities of ST2 and 3 were
535 more similar to each other than to ST1. These results suggest that regardless different
536 functional genes (*nifH*, *nirS* and *nirK*), the structure of the mats and its position in the
537 littoral gradient overwhelmingly drive the diversity of the community, rather than single
538 geochemical factors.

539

540 NirS and NirK nitrite reductases are functionally equivalent, but there is a debate going
541 on as to whether the two types of denitrifiers are ecologically distinct (Jones & Hallin,
542 2010). Smith & Ogram (2008) found that *nirS*- and *nirK*- denitrifiers responded
543 differently to environmental gradients. In this study, we found that *nirS*- and *nirK*-
544 denitrifiers were similarly affected by environmental variables (Fig. 2). However,
545 although this does not exclude the possibility that the two types of denitrifiers inhabit
546 different niches, we have also no evidence for the opposite that they occupy the same
547 niche. Desnues *et al.* (2007) investigated the vertical zonation of *nirS*- and *nirK*-
548 denitrifiers in a hypersaline mat. These authors found that *nirS* was mainly localized in

549 the permanent anoxic layer whereas *nirK* occurred throughout the whole mat and seemed
550 to be better adapted to environmental fluctuations. Shannon index based on *nirS* and *nirK*
551 sequences indicated a higher diversity of *nirS* clones compared to *nirK* clones at station
552 3. This finding agrees with observations from another ecosystem (Mosier & Francis,
553 2010). However, the opposite was found for the stations 1 and 2. The seasonal changes of
554 abundance of *nirS* and *nirK* were not consistent and varied between stations. This would
555 imply that *nirS*- and *nirK*-denitrifiers adapt differently to the environment. As illustrated
556 in a previous study (Santoro *et al.*, 2006), caution is needed because comparisons by
557 using richness estimates may vary according to sample size. The GeoChip results showed
558 a similar diversity and richness for *nirS* and *nirK*. It has been shown that in some
559 ecosystems *nirS*-denitrifiers were more abundant than *nirK*-denitrifiers (Mosier &
560 Francis, 2010). In our study, *nirS*- and *nirK*-denitrifiers were equally abundant in the
561 GeoChip analysis, suggesting that both types of denitrifiers play important roles in
562 denitrification in the microbial mats.

563

564

565 References:

- 566 Bernhard AE, Landry ZC, Blevins A, de la Torre JR, Giblin AE & Stahl DA
567 (2010) Abundance of ammonia-oxidizing archaea and bacteria along an estuarine salinity
568 gradient in relation to potential nitrification rates. *Appl Environ Microbiol* **76**: 1285-1289.
569
- 570 Bolhuis H & Stal LJ (2011) Analysis of bacterial and archaeal diversity in coastal
571 microbial mats using massive parallel 16S rRNA gene tag sequencing. *ISME J* **5**: 1701-
572 1712.
573
- 574 Bolhuis H, Fillinger L & Stal LJ (2013) Coastal microbial mat diversity along a natural
575 salinity gradient. *PLoS ONE* **8(5)**: e63166.
576
- 577 Bonin PC & Michotey VD (2006) Nitrogen budget in a microbial mat in the Camargue
578 (southern France). *Mar Ecol Prog Ser* **322**: 75-84.
579
- 580 Braker G, Zhou JZ, Wu LY, Devol AH & Tiedje JM (2000) Nitrite reductase genes (*nirK*
581 and *nirS*) as functional markers to investigate diversity of denitrifying bacteria in Pacific
582 northwest marine sediment communities. *Appl Environ Microbiol* **66**: 2096-2104.
583
- 584 Bulow SE, Francis CA, Jackson GA & Ward BB (2008) Sediment denitrifier community
585 composition and *nirS* gene expression investigated with functional gene microarrays.
586 *Environ Microbiol* **10**: 3057-3069.
587
- 588 Castro-Gonzalez M, Braker G, Farias L & Ulloa O (2005) Communities of *nirS*-type
589 denitrifiers in the water column of the oxygen minimum zone in the eastern South
590 Pacific. *Environ Microbiol* **7**: 1298-1306.
591
- 592 Cavigelli MA & Robertson GP (2000) The functional significance of denitrifier
593 community composition in a terrestrial ecosystem. *Ecology* **81**: 1402-1414.
- 594 Desnues C, Michotey VD, Wieland A, Zhizang C, Fourcans A, Duran R & Bonin PC
595 (2007) Seasonal and diel distributions of denitrifying and bacterial communities in a
596 hypersaline microbial mat (Camargue, France). *Water Res* **41**: 3407-3419.
597
- 598 Hallin S, Jones CM, Schloter M & Philippot L (2009) Relationship between N-cycling
599 communities and ecosystem functioning in a 50-year-old fertilization experiment. *ISME J*
600 **3**: 597-605.
601
- 602 Hannig M, Braker G, Dippner J & Jürgens K (2006) Linking denitrifier community
603 structure and prevalent biogeochemical parameters in the pelagial of the central Baltic
604 Proper (Baltic Sea). *FEMS Microbiol Ecol* **57**: 260-271.
605
- 606 He ZL, Deng Y, Van Nostrand JD *et al.* (2010) GeoChip 3.0 as a high-throughput tool for
607 analyzing microbial community composition, structure and functional activity. *ISME J* **4**:
608 1167-1179.

609
610 Jayakumar DA, Francis CA, Naqvi SWA & Ward BB (2004) Diversity of nitrite
611 reductase genes (*nirS*) in the denitrifying water column of the coastal Arabian Sea. *Aquat*
612 *Microb Ecol* **34**: 69-78.
613
614 Jones CM & Hallin S (2010) Ecological and evolutionary factors underlying global and
615 local assembly of denitrifier communities. *ISME J* **4**: 633-641.
616
617 Joye SB & Paerl HW (1994) Nitrogen cycling in microbial mats: rates and patterns of
618 denitrification and nitrogen fixation. *Mar Biol* **119**: 285-295.
619
620 Kim O-S, Imhoff J, Witzel K-P & Junier P (2011) Distribution of denitrifying bacterial
621 communities in the stratified water column and sediment–water interface in two
622 freshwater lakes and the Baltic Sea. *Aquat Ecol* **45**: 99-112.
623
624 Liang YT, He ZL, Wu LY, Deng Y, Li GH & Zhou JZ (2010) Development of a
625 Common oligonucleotide reference standard for microarray data normalization and
626 comparison across different microbial communities. *Appl Environ Microbiol* **76**: 1088-
627 1094.
628
629 Liu XD, Tiquia SM, Holguin G, Wu LY, Nold SC, Devol AH, Luo K, Palumbo AV,
630 Tiedje JM & Zhou JZ (2003) Molecular diversity of denitrifying genes in continental
631 margin sediments within the oxygen-deficient zone off the Pacific coast of Mexico. *Appl*
632 *Environ Microbiol* **69**: 3549-3560.
633
634 Lohse L, Kloosterhuis HT, vanRaaphorst W & Helder W (1996) Denitrification rates as
635 measured by the isotope pairing method and by the acetylene inhibition technique in
636 continental shelf sediments of the North Sea. *Mar Ecol Prog Ser* **132**: 169-179.
637
638 McCune B, Grace JB & Urban DL (2002) Analysis of ecological communities, vol. 28.
639 MjM Software Design Gleneden Beach, Oregon.
640
641 Mosier AC & Francis CA (2010) Denitrifier abundance and activity across the San
642 Francisco Bay estuary. *Environ Microbiol Rep* **2**: 667-676.
643
644 Oakley BB, Francis CA, Roberts KJ, Fuchsman CA, Srinivasan S & Staley JT (2007)
645 Analysis of nitrite reductase (*nirK* and *nirS*) genes and cultivation reveal depauperate
646 community of denitrifying bacteria in the Black Sea suboxic zone. *Environ Microbiol* **9**:
647 118-130.
648
649 Oksanen J (2011) Multivariate analysis of ecological communities in R: vegan tutorial. *R*
650 *package version: 2.0-1*.
651
652 Osaka T, Yoshie S, Tsuneda S, Hirata A, Iwami N & Inamori Y (2006) Identification of
653 acetate- or methanol-assimilating bacteria under nitrate-reducing conditions by stable-
654 isotope probing. *Microb Ecol* **52**: 253-266.

655
656 Philippet L & Hallin S (2005) Finding the missing link between diversity and activity
657 using denitrifying bacteria as a model functional community. *Curr Opin Microbiol* **8**:
658 234-239.
659
660 Prieme A, Braker G & Tiedje JM (2002) Diversity of nitrite reductase (*nirK* and *nirS*)
661 gene fragments in forested upland and wetland soils. *Appl Environ Microbiol* **68**: 1893-
662 1900.
663
664 Rich JJ, Heichen RS, Bottomley PJ, Cromack K & Myrold DD (2003) Community
665 composition and functioning of denitrifying bacteria from adjacent meadow and forest
666 soils. *Appl Environ Microbiol* **69**: 5974-5982.

667 Santoro AE, Boehm AB & Francis CA (2006) Denitrifier community composition along
668 a nitrate and salinity gradient in a coastal aquifer. *Appl Environ Microbiol* **72**: 2102-
669 2109.
670
671 Severin I & Stal LJ (2008) Light dependency of nitrogen fixation in a coastal
672 cyanobacterial mat. *ISME J* **2**: 1077-1088.
673
674 Severin I, Acinas SG & Stal LJ (2010) Diversity of nitrogen-fixing bacteria in
675 cyanobacterial mats. *FEMS Microbiol Ecol* **73**: 514-525.
676
677 Severin I & Stal LJ (2010) Spatial and temporal variability in nitrogenase activity and
678 diazotrophic community composition in coastal microbial mats. *Mar Ecol Prog Ser*
679 417:13-25
680
681 Severin I, Confurius-Guns V & Stal LJ (2012) Effect of salinity on nitrogenase activity
682 and composition of the active diazotrophic community in intertidal microbial mats. *Arch*
683 *Microbiol* **194**: 483-491.
684
685 Smith JM & Ogram A (2008) Genetic and functional variation in denitrifier populations
686 along a short-term restoration chronosequence. *Appl Environ Microbiol* **74**: 5615-5620.
687
688 Stal LJ, Grossberger S & Krumbein WE (1984) Nitrogen fixation associated with the
689 cyanobacterial mat of a marine laminated microbial ecosystem. *Mar Biol* **82**: 217-224.
690
691 Stal LJ, Van Gernerden H & Krumbein WE (1985) Structure and development of a
692 benthic marine microbial mat. *FEMS Microbiol Ecol* **31**: 111-125.
693
694 Stal LJ (2001) Coastal microbial mats: the physiology of a small-scale ecosystem. *S Afr J*
695 *Bot* **67**: 399-410.
696
697 Stal LJ (2003) Nitrogen cycling in marine cyanobacterial mats. In: Krumbein WE,
698 Paterson DM, Zavarzin GA (eds). *Fossil and Recent biofilms: a natural history of life on*
699 *Earth*. Springer. pp 119-140.

700

701 Stal LJ (2012) Microbial mats and stromatolites. In: Whitton BA (ed). *Ecology of*
702 *Cyanobacteria II: Their Diversity in Space and Time*, Springer, Dordrecht. pp 65-125.

703

704 Team RDC (2011) R: A language and environment for statistical computing. Vienna,
705 Austria: R Foundation for Statistical Computing; 2008. ISBN 3-900051-07-0. Available
706 at: <http://www.R-project.org>.

707

708 Thamdrup B & Dalsgaard T (2002) Production of N₂ through anaerobic ammonium
709 oxidation coupled to nitrate reduction in marine sediments. *Appl Environ Microbiol* **68**:
710 1312-1318.

711

712 Throbäck IN, Enwall K, Jarvis Å & Hallin S (2004) Reassessing PCR primers targeting
713 *nirS*, *nirK* and *nosZ* genes for community surveys of denitrifying bacteria with DGGE.
714 *FEMS Microbiol Ecol* **49**: 401-417.

715

716 Throbäck IN, Johansson M, Rosenquist M, Pell M, Hansson M & Hallin S (2007) Silver
717 (Ag⁺) reduces denitrification and induces enrichment of novel *nirK* genotypes in soil.
718 *FEMS Microbiol Lett* **270**: 189-194.

719

720 Wu LY, Liu X, Schadt CW & Zhou JZ (2006) Microarray-based analysis of
721 subnanogram quantities of microbial community DNAs by using whole-community
722 genome amplification. *Appl Environ Microbiol* **72**: 4931-4941.

723

724 Yoshie S, Noda N, Tsuneda S, Hirata A & Inamori Y (2004) Salinity decreases nitrite
725 reductase gene diversity in denitrifying bacteria of wastewater treatment systems. *Appl*
726 *Environ Microbiol* **70**: 3152-3157.

727

728 Zumft W (1997) Cell biology and molecular basis of denitrification. *Microbiol Mol Biol*
729 *Rev* **61**: 533-616.

730

731

732

733

734

735 Acknowledgments

736 This work was financially supported by the Dutch Organization for Scientific Research,
737 Earth and Life Science (NWO-ALW) grant 839.08.332. The authors are indebted to Dr.
738 Jizhong (Joe) Zhou and his team at the University of Oklahoma for hosting HF to carry
739 out the GeoChip analyses. We also thank Veronique Confurius and Dr. Juliette Ly for
740 their help with the fieldwork.

741

742

743 Tables:

744 Table 1. The geographical coordinates and description of the mats investigated in this

745 study.

Station	Geographical coordinates	Description
Station 1 (ST1)	53°29.445'N, 6°8.718'E	Mainly freshwater influenced site, close to the dunes. Irregularly inundated.
Station 2 (ST2)	53°29.460'N, 6°8.309'E	Seawater influenced site, developing microbial mat. At the low water mark.
Station 3 (ST3)	53°29.445'N, 6°8.342'E	Seawater and freshwater influenced site, located between ST1 and ST2, at the edge of the salt marsh

746

747
748

Table 2. Physicochemical parameters and potential denitrification rates in the microbial mats during the 2010 sampling period.

	July (2010)	September (2010)	January (2010)	April (2011)
Station 1				
Temperature (°C, sediment)	17	10	0	8
NH ₄ ⁺ (μmol/l)	128.9±3.0	83.7±17.3	191.3±23.4	233.1±23.7
NO _x ⁻ (μmol/l)	23.3±4.6	8.4±1.1	9.6±4.6	25.9±3.4
PO ₄ ³⁻ (μmol/l)	20.1±6.1	3.1±0.5	n.d.	25±3.8
TOC (%)	0.04	0.06	0.04	0.04
TN (%)	0.006	0.01	0.007	0.007
C/N	6.7	6.0	5.7	5.7
Salinity (psu)	18	19	15	17
Denitrification (mmol N m ⁻² d ⁻¹)	7.0±1.0	1.6±0.3	2.4±0.3	0.1±0.05
Station 2				
Temperature (°C, sediment)	17	10	0	8
NH ₄ ⁺ (μmol/l)	587.9±41.2	216.2±69.8	736.8±199.6	486.1±61.3
NO _x ⁻ (μmol/l)	22.4±14.7	8.7±1.4	6.2±1.1	20.6±4.5
PO ₄ ³⁻ (μmol/l)	19.7±2.0	3.2±0.9	n.d.	58.6±26.3
TOC (%)	0.19±0.01	0.20±0.03	0.20±0.03	0.17±0.02
TN (%)	0.03	0.04	0.03	0.03
C/N	6.3	5.0	6.7	5.7
Salinity (psu)	28	28	30	28
Denitrification (mmol N m ⁻² d ⁻¹)	0.1±0.05	0.1±0.05	1.6±0.4	0.2±0.1
Station 3				
Temperature (°C, sediment)	17	10	0	8
NH ₄ ⁺ (μmol/l)	217.3±102.3	255.9±68.4	510.2±62.2	475.8±3.5
NO _x ⁻ (μmol/l)	16.0±3.7	7.6±1.9	2.8±0.6	19.6±4.0
PO ₄ ³⁻ (μmol/l)	28.5±15.2	3.9±1.2	n.d.	48.5±10.6
TOC (%)	0.11±0.03	0.15±0.02	0.15±0.02	0.13±0.02
TN (%)	0.02	0.03	0.03	0.02
C/N	5.5	5.0	5.0	6.5
Salinity (psu)	25	25	22	23
Denitrification (mmol N m ⁻² d ⁻¹)	0.7±0.2	0.1±0.05	0.5±0.2	0.1±0.05

749

Abbreviations: n.d., no data; TOC, total organic carbon; TN, Total nitrogen.

750 Table 3. Richness and diversity statistics of *nirS* and *nirK* clone libraries based on 95%
751 cutoffs.

752

	No. of clones	No. of OTUs	ACE	Chao1	Shannon	Simpson
<i>nirS</i>						
ST1	55	20	56	42	2.1	0.25
ST2	48	19	131	49	2.2	0.18
ST3	66	32	48	47	3.2	0.03
<i>nirK</i>						
ST1	70	35	481	194	3.3	0.05
ST2	69	27	122	84	2.6	0.18
ST3	52	17	41	30	2.1	0.13

753

754

755

756 Table 4. Summary of *nirS* and *nirK* genes detected by GeoChip, including the number
 757 and percentage of overlapping (*italic*) and unique (**bold**) sequences, the diversity indices
 758 and abundance for each station.

	ST1_July	ST2_July	ST3_July	ST1_Jan.	ST2_Jan.	ST3_Jan.
<i>nirS</i>						
ST1_July	26(10.3%)	<i>200(77.2%)</i>	<i>144(56.5%)</i>	<i>210(81.4%)</i>	<i>159(62.4%)</i>	<i>124(48.8%)</i>
ST2_July		3(1.5%)	<i>145(70.1%)</i>	<i>185(78.4%)</i>	<i>154(72.3%)</i>	<i>123(59.1%)</i>
ST3_July			1(0.7%)	<i>139(62.6%)</i>	<i>123(66.9%)</i>	<i>112(70.4%)</i>
ST1_Jan.				3(1.4%)	<i>161(74.9%)</i>	<i>124(57.4%)</i>
ST2_Jan.					0(0.00%)	<i>116(68.2%)</i>
ST3_Jan.						0(0.00%)
Richness*	253	206	146	215	161	125
Shannon-Weaver (H)	5.5	5.3	5	5.4	5.1	4.8
Abundance (%)**	8.2	7.7	7.4	7.9	7.8	7.4
<i>nirK</i>						
ST1_July	26(10.2%)	<i>200(76.9%)</i>	<i>139(53.9%)</i>	<i>212(82.2%)</i>	<i>147(56.8%)</i>	<i>124(47.9%)</i>
ST2_July		1(0.5%)	<i>139(67.5%)</i>	<i>184(78.6%)</i>	<i>144(68.6%)</i>	<i>126(61.5%)</i>
ST3_July			1(0.7%)	<i>134(60.6%)</i>	<i>117(67.2%)</i>	<i>116(76.3%)</i>
ST1_Jan.				1(0.5%)	<i>145(66.2%)</i>	<i>122(55.7%)</i>
ST2_Jan.					1(0.7%)	<i>116(72.1%)</i>
ST3_Jan.						0(0.00%)
Richness *	256	204	141	214	150	127
Shannon-Weaver (H)	5.5	5.3	4.9	5.4	5	4.8
Abundance (%)**	8.3	7.6	7.3	7.9	7.3	7.6

759 * richness was determined as probe numbers detected.

760 **abundance was determined by dividing the hybridization intensity of *nirS* or *nirK* on the GeoChip by the
 761 total signal of all nitrogen cycling genes detected on the array.

762

763

764 Table 5. MRPP A-values of the denitrifier community composition.

Difference between group		
Spatial differences	A-value (clone library)	A-value (GeoChip)
<i>nirS</i>		
ST1 vs ST2	0.753 (p=0.024)*	0.190 (p=0.002)*
ST1 vs ST3	0.749 (p=0.018)*	0.400 (p=0.001)*
ST2 vs ST3	0.667 (p=0.027)*	0.059 (p=0.108)
<i>nirK</i>		
ST1 vs ST2	0.604 (p=0.029)*	0.242 (p=0.004)*
ST1 vs ST3	0.721 (p=0.045)*	0.454 (p=0.002)*
ST2 vs ST3	0.501 (p=0.020)*	0.66 (p=0.096)

765 * means p<0.05 (statistical difference between whole *nirS* and *nirK* profiles assessed using multi-response
 766 permutation procedure).

767

768

769 Legends

770

771 Figure 1. Phylogenetic trees for *nirS* (A) and *nirK* (B) genes, based on the translated
772 amino acid sequence, constructing by neighbor-joining method in MEGA 5. Sequences
773 from this study were shown as the percentage of environmental clones from each station.
774 Significant bootstrap values (>50) are shown at branch nodes.

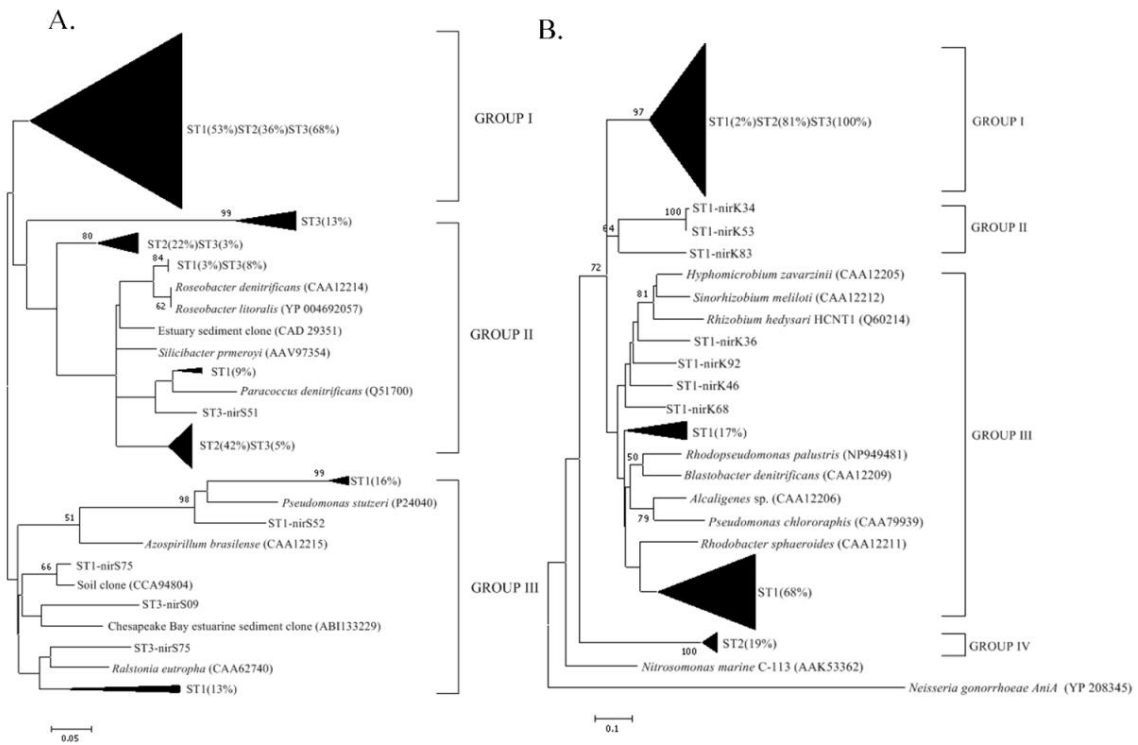
775 Figure 2. Canonical correspondence analysis of the denitrifier community composition of
776 mat samples. (A) and (C): analysis based on *nirS* and *nirK* clone data and points represent
777 the denitrifier community from seasonal samples at indicated station. (B) and (D):
778 analysis based on *nirS* and *nirK* GeoChip data and points represent replicated denitrifier
779 community from summer and winter samples at indicated station (S: summer; W:
780 winter). Arrows represent the relationship between environmental parameters with the
781 denitrifier communities.

782

783

784 Figures:

785 Fig. 1



786

787

788

789

790

791

792

793

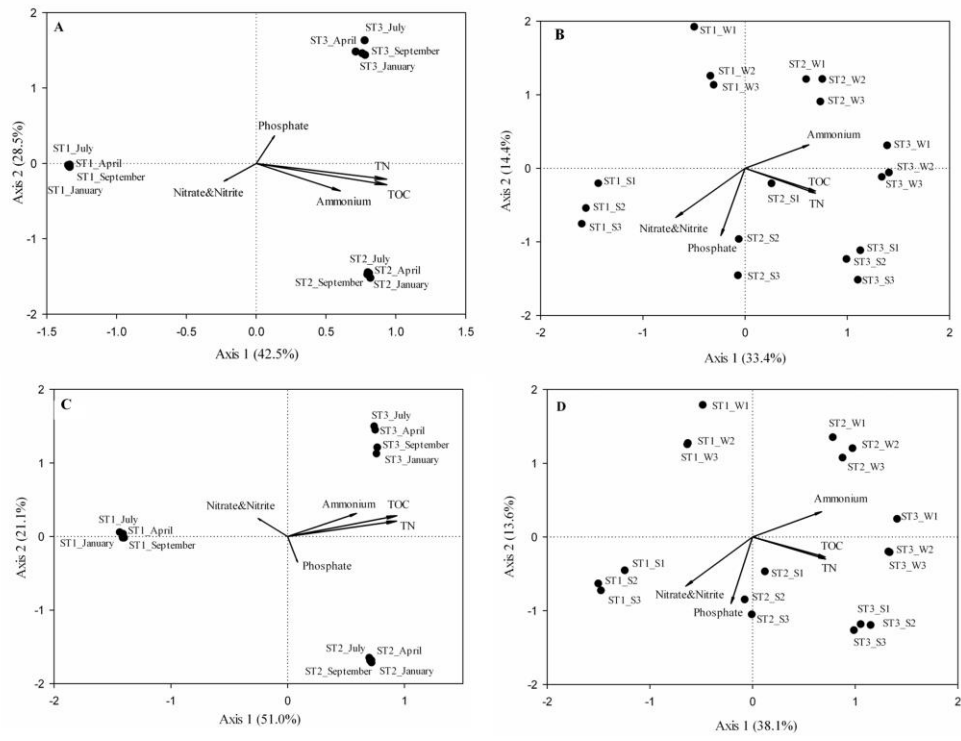
794

795

796

797

798 Fig. 2



799

800